

Bistatic GMTI Experiment for Airborne Platforms

Pileih Chen, *Member, IEEE*, and James K. Beard, *Member, IEEE*

Abstract—The concept of bistatic ground moving target indicator BGMTI is presented here. Monostatic GMTI radars use separate modes for ground movers whose Doppler does and does not allow separation of the target return from ground clutter using frequency processing. Bistatic flight scenarios that minimize Doppler spreading in the vicinity of a designated target area are presented as candidate flight test plans. Flight scenarios supporting a sustained broadside spot mode and an oblique spot mode are presented.

Index terms— bistatic GMTI BGMTI surveillance radar

I. INTRODUCTION

Bistatic ground moving target indicator (BGMTI) is useful for detection and tracking of both slow and fast ground movers. Conventional monostatic ground moving target indicator (GMTI) radars use a separate mode for ground movers whose Doppler does not allow separation of their return from ground clutter using frequency processing. This is endoclobber processing, and is designed to detect ground movers whose Doppler is contained within the bandwidth of ground clutter. Exoclobber radar modes and processing are designed to detect ground movers whose Doppler is outside the ground clutter Doppler bandwidth. Exoclobber modes are similar to airborne lookdown pulse Doppler radar modes and processing except that the target Doppler is much lower.

Ground clutter Doppler bandwidth is determined by the antenna azimuth beamwidth, the squint angle of the beam boresight, and the platform ground speed. Endoclobber processing is challenging because ground clutter Doppler bandwidth is often broad enough so that ground movers of interest are well within it. The extra freedom allowed by defining bistatic radar operation allows more control over the clutter spectral regions relative to the Doppler of ground movers. Proper choice of flight geometries produces smaller Doppler spreading of ground clutter returns. Thus, by use of pre-determined flight geometries, lower minimum detectable velocity (MDV) can be achieved for ground movers using BGMTI radars than is possible for monostatic GMTI radars. We show here how this technique can be used to exploit the BGMTI trade space to achieve lower

MDV than that of otherwise similar monostatic GMTI radars.

II. BISTATIC SHIFT AND SPREAD

The bistatic Doppler shift resulting from two moving platforms is defined by equation (1), based on a generic bistatic geometry shown in Figure 1 which was intended for bistatic SAR mapping.

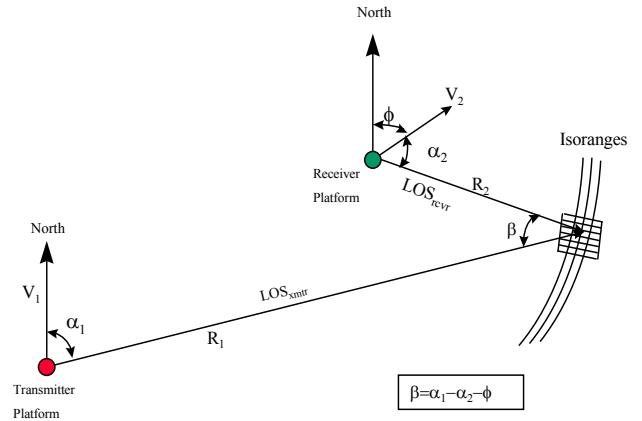


Figure 1 Bistatic Flying Geometry to Measure Clutter Doppler and Spread

$$f_d = -\left(\frac{\dot{R}_1}{\lambda} + \frac{\dot{R}_2}{\lambda}\right) \quad (1)$$

$$= \frac{V_1}{\lambda} \cos \alpha_1 + \frac{V_2}{\lambda} \cos \alpha_2$$

where:

f_d = bistatic Doppler shift,

\dot{R}_1 = transmitter velocity,

\dot{R}_2 = receiver velocity,

λ = RF wavelength,

α_1 = angle between transmitter velocity vector and transmitter's line-of-sight (LOS),

α_2 = angle between receiver velocity vector and receiver's LOS,

V_1 = transmitter platform's velocity,

V_2 = receiver platform's velocity,

β = bistatic angle,

ϕ = receiver velocity angle off the North,

R_1 = transmitter-to- ground range, and
 R_2 = receiver-to-ground range.

A vector notation approach is important here because it does not use approximations and also its simplicity of implementation in three dimensional scenarios. The bistatic Doppler as given in equation (1) is

$$f_d = -\frac{1}{\lambda} \frac{d}{dt} (R_1 + R_2) \quad (2)$$

$$= \frac{1}{\lambda} (\underline{ur}_1^T \underline{v}_1 + \underline{ur}_2^T \underline{v}_2)$$

where the ranges from the vector platform locations \underline{p}_i to the ground target location \underline{s} are

$$R_i^2 = \underline{r}_i^T \cdot \underline{r}_i, \quad \underline{r}_i = \underline{s} - \underline{p}_i, \quad i = 1, 2. \quad (3)$$

The underline denotes a column vector. The range rates given in equations (1) and (2), are found by differentiating equation (3) with respect to time, are

$$\dot{R}_i = -\underline{ur}_i^T \cdot \underline{v}_i \quad (4)$$

where \underline{v}_i is the velocity of platform i and \underline{ur}_i is the unit pointing vector from platform i ,

$$\underline{ur}_i = \frac{\underline{r}_i}{R_i}, \quad i = 1, 2. \quad (5)$$

The rate of change of bistatic Doppler over distance is a measure of Doppler spreading. This gradient times the extent of the illuminated area is an approximation of the Doppler spreading of ground clutter. The gradient of Doppler with respect to position \underline{s} of the ground scatterer is

$$\frac{\partial f_d}{\partial \underline{s}} = \frac{1}{\lambda} \left[\frac{1}{R_1} B_1 \cdot \underline{v}_1 + \frac{1}{R_2} B_2 \cdot \underline{v}_2 \right]. \quad (6)$$

The matrices B_i are the subspace operators that, considered as an operator on a vector, removes the components of that vector along the line of sight from platform i :

$$B_i = I - \underline{ur}_i \cdot \underline{ur}_i^T. \quad (7)$$

Note the convention used here for the vector inner product or dot product, and the vector outer product.

This vector gradient of Doppler with respect to ground position is the sum of the vector angle rates of the platforms as seen from the target, divided by wavelength. These vector angle rates are the platform velocity vector projected on the plane across the line of sight, divided by slant range. The magnitude of this vector is the change in Doppler over an illuminated area in Hz per meter of distance along the direction of the vector. IsoDoppler contours are normal to this vector.

The form of equation (6) suggests that Doppler spreading can be minimized or driven to zero by proper selection of flight geometry.

The significance of reducing the Doppler spreading to zero or close to zero is illustrated in Figure 2. For a monostatic radar, a slow moving target is most probably masked by the

main lobe clutter spread; while for a bistatic radar, the same moving target can become an exoclutler target when the bistatic clutter tuning technique is optimally applied. As a result, the minimum detectable velocity (MDV) will be limited only by receiver thermal noise.

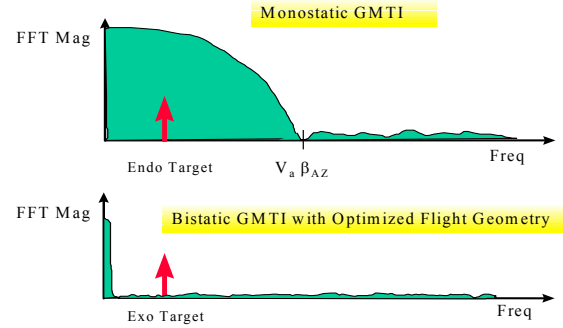


Figure 2 BGMTI Utilizes Clutter Tuning Technique to Make the Same Slow Moving Target Moving Target More Detectable than a Conventional Monostatic Radar [V_a = Aircraft Ground Speed, β_{AZ} = Antenna Azimuth Beamwidth]

From equation (6), we can show that velocities for the receiver which will give a zero Doppler spread are of the form:

$$\underline{v}_2 = -\frac{R_2}{R_1} \cdot B_2 \cdot B_1 \cdot \underline{v}_1 + c \cdot \underline{ur}_2 \quad (8)$$

where c is the component of the receiver velocity \underline{v}_2 along the line of sight from the receiver to the target. This is a solution in a least squares sense, and is the best we can do with only \underline{v}_2 as a free variable. This is because the matrix B_2 is singular so that a strict solution of equation (6) for \underline{v}_2 that drives the right hand side to zero does not exist.

Substituting \underline{v}_2 as obtained from equation (8) into equation (6) shows that this minimum velocity spreading gradient is

$$\left(\frac{\partial f_d}{\partial \underline{s}} \right)_{MIN} = \frac{1}{\lambda R_1} (\underline{ur}_2 \underline{ur}_2^T) B_1 \underline{v}_1 \quad (9)$$

$$= \frac{1}{\lambda R_1} \left((\underline{ur}_2^T \underline{v}_1) + \dot{R}_1 \cos(\beta) \right) \underline{ur}_2$$

Note that c does not appear, because components of \underline{v}_2 along the line of sight from the receiver to the target do not affect bistatic Doppler. The bistatic angle β is the angle between the lines of sight from the transmitter and receiver,

$$\cos(\beta) = \underline{ur}_1^T \underline{ur}_2. \quad (10)$$

Examination of the minimum Doppler spreading as given in the first form of equation (9) and the allowable receiver velocities in equation (8) shows that the velocity spreading in the vicinity of the target can be driven to zero, exactly, only if

1. The lines of sight from the transmitter and receiver to the target area are orthogonal, and the receiver must fly along its line of sight with the target,
2. Both the transmitter and receiver are flying along the line of sight, or
3. The component of \underline{v}_1 across the line of sight from the transmitter to the target area is orthogonal to the line of sight from the receiver to the target area, and the receiver velocity is the negative of this vector plus an arbitrary component along the line of sight from the receiver to the target.

Condition 1, in the first form in equation (9), leads to a product of zero between the vector outer product in parentheses and the matrix B_1 . Examining this case in three dimensions and constraining the receiver to fly at a constant altitude shows that this condition is best honored as an approximation. An opportunity to exploit this geometry for a few minutes can be taken by illuminating a target area ahead of a receiver BGMTI platform when the transmitter line of sight to the target area is normal to the receiver path.

Condition 2 follows from a zero product of B_1 and \underline{v}_1 , and leads to a condition of constant frequency. Examining this case in three dimensions and constraining the transmitter to fly at a constant altitude shows that this condition is best honored as an approximation, in which case the area directly ahead of the transmitter are favored. This geometry can be exploited by illuminating a target area near the point where the ground tracks of the transmitter and receiver cross. Note, however, that ground Doppler spreading is also minimized when either platform is used for monostatic GMTI.

Condition 3 follows from orthogonality of the product of B_1 and \underline{v}_1 and the line of sight from the receiver to the target area. A spot mode can be constructed using this geometry by having both transmitter and receiver fly in a circle around the target area, both clockwise or both counterclockwise, maintaining a bistatic angle of 180 degrees, neglecting elevation. Such a flight geometry is shown in Figure 3. Generalizations are possible such as elliptical flight paths, and straight flight paths in which the target area is between them.

There are two values of c in (9) that give the same magnitude for \underline{v}_2 anywhere in the circular receiver flight path in Figure 3 as that for a zero bistatic angle. One of them is the exact same \underline{v}_2 that applies for a zero bistatic angle,

$$\underline{v}_2 = -\frac{R_2}{R_1} \underline{v}_1, \beta = 0. \quad (15)$$

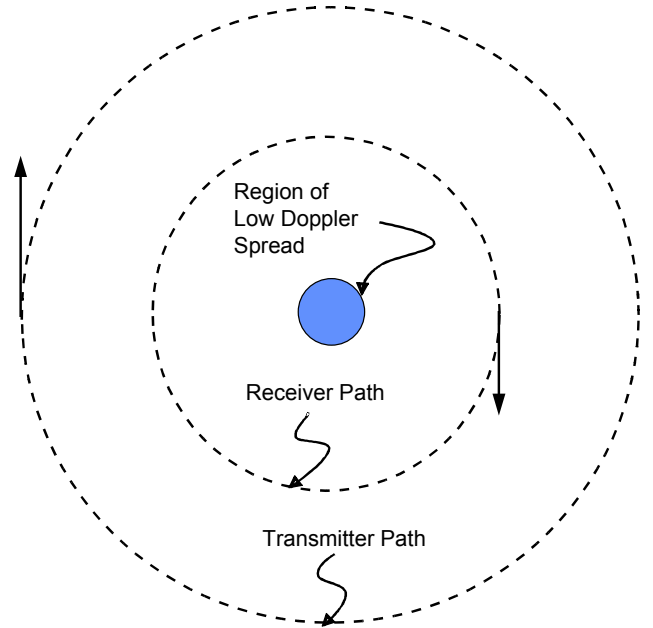


Figure 3 Top View of Flight Geometry for the Spot Mode BGMTI

The other is its mirror image in a plane normal to the line of sight from the receiver to the target. Unfortunately, neither of these is, in general, aligned with the locus of the flight path, even neglecting elevation. They produce a nonzero Doppler spreading. The Doppler spreading or the two values is compared in the plot shown in Figure 4 for the flight profile in Table 1.

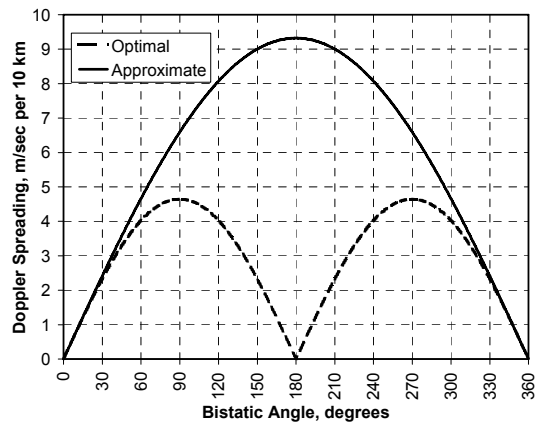


Figure 4 Counterrotating Circular Transmitter and Receiver Vehicle Flight Paths Approximate Optimal Doppler Spreading over Portion of Flight Path

A set of contours of Doppler spreading for a monostatic case using only the transmitter is shown in Figure 5.

Table 1 Operational System Parameters for GMTI Experiment

Operating Parameter	Nominal Value	Comments
Transmitter platform velocity	300 knots	Maintain $V_1/R_1 = V_2/R_2$ Ratio & Velocity Vector
Receiver platform velocity	180 knots	
Transmitter-to-ground range	330 km	
Receiver-to-ground range	198 km	
Ground target velocity	2, 4, 20, 20 knots	
Target velocity bisector angle	0 to 90 degrees	No Doppler Shift at 90 degrees
Transmitter LOS Angle	90 degrees	Counter-rotating Flight Path
Receiver LOS Angle	90 degrees	Counter-rotating Flight Path
Target RCS	5 square meters	Nominal Value

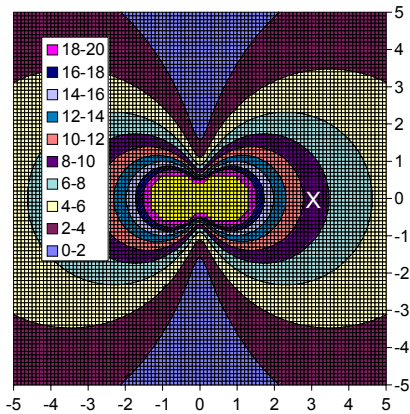


Figure 5 Contours of Monostatic Doppler Spreading in m/sec per 10 km of distance. Axes are in degrees of great circle arc, or about 111 km per degree. The X locates a broadside target at 330 km.

Figure 4 shows that the worst case Doppler spreading is approximately 9.5 meters per second over a 10 km ground extent, about the same as for the monostatic case as shown in Figure 5, so that the data taken in the flight test can be used to show contrasts in use of flight patterns that minimize Doppler spread. Figure 6 shows contours of Doppler spreading for flight parameters as given in Table 1, with a two dimensional bistatic angle of 180 degrees. Note that, as time increases, this geometry rotates but all angles remain the same. Thus this geometry is suitable for sustained surveillance of a fixed area -- a spot mode BGMTI.

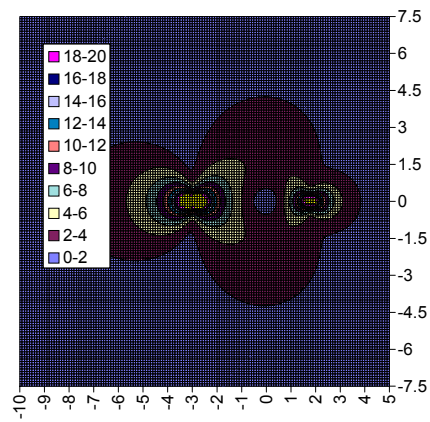


Figure 6 Contours of Doppler spreading for the flight parameters of Table 1 show low Doppler spreading at the target area at (0, 0).

Figure 7 shows contours for two platforms closing on one another with each 45 degrees off the nose of the other. This configuration exploits condition 3. Note the large S shaped area between them with low Doppler spreading.

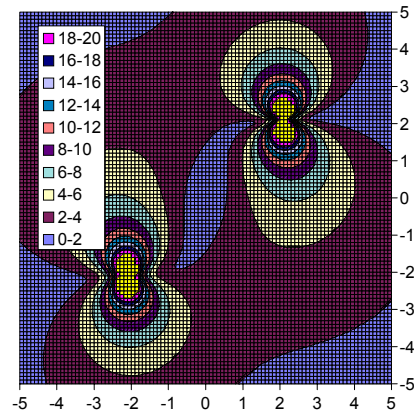


Figure 7 Doppler spreading contours for a 45 degree squint angle and a bistatic angle of 180 degrees. Flight parameters are those in Table 1.

III. BGMTI CONCEPTUAL EXPERIMENT

Figure 3 above depicts an optimum BGMTI for the spot mode, or so called broadside MTI, in which transmitter and receiver fly circular paths about a ground target. The purpose of flying such a geometry is to attempt to cancel clutter spread originated from each platform. To reduce the total number of bistatic parameters, the velocity vector of the transmitter or the receiver is kept perpendicular to the corresponding line-of-sight vector, and the target is kept between the transmitter and receiver. Given such a geometry, the next constraint is to keep the crossrange velocity to range ratio of V_1/R_1 the same as V_2/R_2 . When such a condition is met, the transmitter's Doppler spread will cancel the receiver's Doppler spread at the point of the target, and the net clutter spread collapses into a single line located at zero Doppler. Some Doppler spreading will

occur due to the illumination of ground clutter near the target where Doppler spreading does not completely cancel.

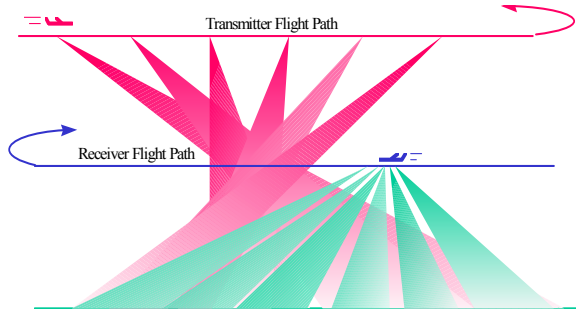


Figure 8 Side View of Flight Geometry for Squinted BGMTI

Figure 8 illustrates the BGMTI for a squinted geometry which provides a larger area of compressed clutter Doppler as compared with the spot mode, as shown in Figure 7. Except for the mid point of the run, the angle between the velocity vector and the LOS is non-orthogonal and clutter Doppler spread tends to be larger than that of the spot mode.

Mission planning objectives are

1. Relatively simple bistatic flight geometry that minimize bistatic clutter return to the receiver.
2. Maintain a constant SNR during the BGMTI flight due to two constant radii, R_1 and R_2 , and receiver thermal noise only performance.
3. Simplify radar timing and receiver gain control design due to a constant bistatic baseline, two constant radii (R_1 and R_2), and a constant SIR.

Item (2) is further analyzed via the bistatic radar range equation, speed-to-range ratio, and receiver thermal noise only performance.

Integrated bistatic SNR_I is:

$$SNR_I = \frac{P_{av} G_1 G_2 \lambda^2 \sigma_T \tau_d}{(4\pi)^3 (kT_0 F) R_1^2 R_2^2 L_S L_R} \quad (16)$$

where:

- P_{av} = average transmitter power,
- G_1 = transmitter antenna gain,
- G_2 = receiver antenna gain,
- σ_T = bistatic target RCS,
- τ_d = coherent integration time,
- k = Boltzman's constant,
- T_0 = receiver system temperature,
- F = receiver noise figure,
- R_1 = transmitter-to-ground range,
- R_2 = receiver-to-ground range,
- L_S = system loss,
- L_R = RF loss,

and speed-to-range ratio is:

$$\frac{V_1}{R_1} = \frac{V_2}{R_2} \quad (17)$$

By substituting R_1 from (17) into (16) and solving for V_2 as a function other bistatic radar parameters:

$$V_2^2 = \frac{SNR_I (4\pi)^3 V_1^2 R_2^4 (kT_0 F) L_S L_R}{P_{av} G_1 G_2 \lambda^2 \sigma_T \tau_d} \quad (18)$$

Using equation (18), receiver velocity V_2 is plotted, in Figure 9, against receiver range R_2 for three transmitter velocities. Table 1 has a set of BGMTI operational parameters for the spot mode. Under a realistic operating scenario, the transmitter's range and velocity are usually pre-determined. If the receiver is on-board a UAV, it would be more flexible in choosing velocity-to-range ratio to maximize the overall performance.

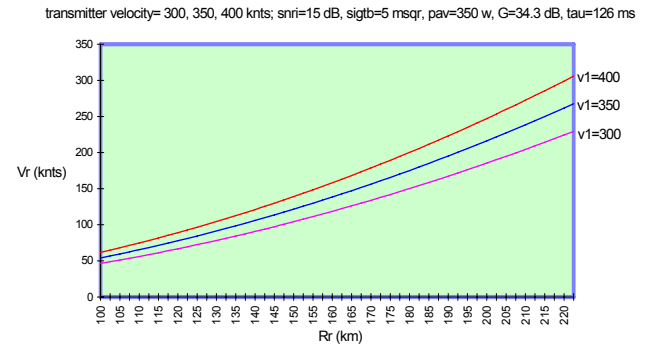


Figure 9 Receiver Range and Velocity Selection Curves for Constant SIR Operation

IV. CONCLUSIONS

Two BGMTI modes, sustained spot and squinted, are developed for a future BGMTI experiment. For the spot mode BGMTI, the bistatic radar equation and minimization of bistatic Doppler spreading are used to determine optimum bistatic system parameters to minimize bistatic main lobe clutter for slow moving target detection. For demonstration, Table 1 has a summary of recommended bistatic flight path parameters for the spot BGMTI experiment.